

# Non-Fermi-Liquid Transport Phenomena and Superconductivity Driven by Orbital Fluctuations in Iron Pnictides: Analysis by Fluctuation-Exchange Approximation

Seiichiro ONARI<sup>1</sup>, and Hiroshi KONTANI<sup>2</sup>

<sup>1</sup> *Department of Applied Physics, Nagoya University and JST, TRIP, Furo-cho, Nagoya 464-8602, Japan.*

<sup>2</sup> *Department of Physics, Nagoya University and JST, TRIP, Furo-cho, Nagoya 464-8602, Japan.*

(Dated: September 21, 2018)

We study the five-orbital Hubbard model including the charge quadrupole interaction for iron pnictides. Using the fluctuation-exchange approximation, orbital fluctuations evolve inversely proportional to the temperature, and therefore the resistivity shows linear or convex  $T$ -dependence for a wide range of temperatures. We also analyze the Eliashberg gap equation, and show that an  $s$ -wave superconducting state without sign reversal ( $s_{++}$ -wave state) emerges when the orbital fluctuations dominate over the spin fluctuations. When both fluctuations are comparable, their competition gives rise to a nodal  $s$ -wave state. The present study offers us a unified explanation for both the normal and superconducting states.

PACS numbers: 74.20.-z, 74.20.Fg, 74.20.Rp

## I. INTRODUCTION

The many-body electronic states and the pairing mechanism in iron pnictides have been significant open problems. By taking account of the Coulomb interaction and the nesting of the Fermi surfaces (FSs) in Fig. 1(a), a fully-gapped sign-reversing  $s$ -wave state ( $s_{\pm}$ -wave state) had been proposed<sup>1-5</sup>. Experimentally, both  $T_c$  and antiferro (AF) spin correlation increases as  $x$  decreases in  $\text{BaFe}_2(\text{As}_{1-x}\text{P}_x)_2$ <sup>6</sup>. In contrast,  $T_c$  in  $\text{LaFeAsO}_{1-x}\text{F}_x$  at  $x = 0.14$  increases from 23 K to 43 K by applying the pressure, whereas AF spin correlation is almost unchanged<sup>7</sup>. Thus, the relationship between  $T_c$  and strength of the spin fluctuation seems to depend on compounds.

On the other hand, an orbital-fluctuation-mediated  $s$ -wave state without sign reversal ( $s_{++}$ -wave state) had been proposed based on the five-orbital Hubbard model including the charge quadrupole interaction<sup>8-12</sup>. The charge quadrupole interaction is induced by the vertex correction (VC)<sup>8</sup> due to the Coulomb interaction and the electron-phonon ( $e$ -ph) interaction due to Fe-ion Einstein oscillations. Within the random-phase-approximation (RPA), it was found that  $d$ -orbital fluctuation is induced by small  $e$ -ph interaction. Especially, the empirical relationship between  $T_c$  and the As-Fe-As bond angle (Lee plot)<sup>13</sup> has been naturally explained. Recently, theoretically predicated orbital fluctuations<sup>9,10</sup> have been detected via the substantial softening of the shear modulus<sup>14</sup>. The softening of the shear modulus and the structure transition have been explained by the two-orbion mechanism based on the orbital fluctuation theory<sup>12</sup>. The  $s_{++}$ -wave state is consistent with the robustness of  $T_c$  against randomness<sup>15-17</sup> as well as the ‘‘resonance-like’’ peak structure in the neutron inelastic scattering<sup>18</sup>.

However, spin/orbital fluctuations obtained by the RPA are reduced by the self-energy correction. Therefore, in order to confirm the orbital fluctuation scenario, it is desired to analyze the many-body electronic

states beyond the RPA. For this purpose, the fluctuation-exchange (FLEX) approximation<sup>19</sup> would be appropriate, in which the absence of spin/orbital order in 2D systems, known as the Mermin-Wagner theorem, is rigorously satisfied<sup>20</sup>.

In this paper, we analyze the five-orbital Hubbard model including the charge quadrupole interaction for iron pnictides using the FLEX approximation.<sup>21</sup> In the normal state, large orbital fluctuations induce highly anisotropic quasiparticle lifetime on the FSs as well as the  $T$ -linear or  $T$ -convex resistivity  $\rho$ <sup>22-24</sup> and the large negative thermo-electric power  $S$ . The large orbital fluctuations also introduce the  $s_{++}$ -wave superconducting (SC) state for a wide range of parameters, and the competition between orbital and spin fluctuations lead to the nodal  $s$ -wave state. We propose that the orbital fluctuation is the origin of both the  $s_{++}$ -wave SC state and the non-Fermi-liquid transport phenomena in the normal state.

## II. FORMULATION

In this paper, we set the  $x$  and  $y$  axes parallel to the nearest Fe-Fe bonds and the orbital  $z^2$ ,  $xz$ ,  $yz$ ,  $xy$  and  $x^2 - y^2$  orbitals are denoted as 1, 2, 3, 4 and 5, respectively.

We employ the five-orbital Hubbard model<sup>1</sup> including the quadrupole-quadrupole [electron-electron (el-el)] interaction induced by the VC due to the Coulomb interaction and  $e$ -ph interaction due to Fe-ion Einstein optical modes. The quadrupole-quadrupole interaction is given as<sup>12</sup>

$$\hat{V}(\omega_n) = -g(\omega_n) \sum_i \left( \hat{O}_{xz}^i \hat{O}_{xz}^i + \hat{O}_{yz}^i \hat{O}_{yz}^i + \hat{O}_{xy}^i \hat{O}_{xy}^i \right), \quad (1)$$

where  $\hat{O}_{\Gamma}^i$  ( $\Gamma = xz, yz, xy$ ) is the charge quadrupole operator and  $g(\omega_n) = g\omega_{\text{D}}^2/(\omega_n^2 + \omega_{\text{D}}^2)$  is proportional to the phonon Green function;  $g = g(0)$  is the effective el-el interaction for  $\omega_n = 0$ , and  $\omega_{\text{D}}$  is the cutoff

frequency<sup>9</sup>. For example, we show non-zero  $V_{ll',mm'}$  for  $l, l', m, m' = 2, 3, 4$  in Fig. 1(b). Other than Fig. 1(b),  $\hat{V}$  has many non-zero off-diagonal elements as explained in Ref.<sup>10,12</sup>, since the Fe-ion oscillation (non- $A_{1g}$  mode) induces various inter-orbital transitions.

In the FLEX approximation<sup>19</sup>, the  $5 \times 5$  self-energy matrix  $\hat{\Sigma}$  in the orbital representation is given by

$$\Sigma_{l_1 l_3}(k) = \frac{T}{N} \sum_q \sum_{l_2 l_4} V_{l_1 l_2, l_3 l_4}^\Sigma(q) G_{l_2 l_4}(k-q), \quad (2)$$

where  $l_i$  represents the orbital,  $N$  is the number of  $\mathbf{k}$  meshes, and we denote  $k = (\mathbf{k}, \epsilon_n)$  with fermion Matsubara frequency  $\epsilon_n = (2n+1)\pi T$ , and  $q = (\mathbf{q}, \omega_n)$  with boson Matsubara frequency  $\omega_n = 2n\pi T$ .

$\hat{G}$  is the  $5 \times 5$  Green function matrix in the orbital basis, and  $\hat{V}^\Sigma$  is the  $25 \times 25$  interaction term for the self-energy given as<sup>25</sup>

$$\begin{aligned} \hat{V}^\Sigma(q) &= \frac{3}{2} \hat{\Gamma}^s \hat{\chi}^s(q) \hat{\Gamma}^s + \frac{1}{2} \hat{\Gamma}^c \hat{\chi}^c(q) \hat{\Gamma}^c \\ &- \frac{1}{4} (\hat{\Gamma}^s - \hat{\Gamma}^c) \hat{\chi}^{\text{irr}}(q) (\hat{\Gamma}^s - \hat{\Gamma}^c) + \frac{3}{2} \hat{\Gamma}^s + \frac{1}{2} \hat{\Gamma}^c(3) \end{aligned}$$

where the irreducible susceptibility is given by

$$\chi_{l_1 l_2, l_3 l_4}^{\text{irr}}(q) = -\frac{T}{N} \sum_k G_{l_1 l_3}(k+q) G_{l_4 l_2}(k), \quad (4)$$

and the spin (orbital) susceptibility is obtained as

$$\hat{\chi}^{s(c)} = \frac{\hat{\chi}^{\text{irr}}}{1 - \hat{\Gamma}^{s(c)} \hat{\chi}^{\text{irr}}}. \quad (5)$$

Here,  $\hat{\Gamma}^s = \hat{S}$  [ $\hat{\Gamma}^c = -\hat{C} - 2\hat{V}(\omega_n)$ ] is the irreducible vertex for the spin [charge] channel;  $\hat{S}$  and  $\hat{C}$  represent the Coulomb interaction in the multiorbital model introduced in Refs.<sup>1,9,10,25</sup>; Their matrix elements consist of the intra-orbital Coulomb  $U$ , the inter-orbital Coulomb  $U'$ , Hund's coupling  $J$  and the pair hopping  $J'$ . We assume that  $J = J'$  and  $U = U' + 2J$ . Since the Fe-ion oscillation induces various inter-orbital transitions, the substantial orbital fluctuations appear at low frequencies. On the other hand, the charge susceptibility  $\chi^c(\mathbf{q}) = \sum_{lm} \chi_{ll',mm}^c(\mathbf{q})$  is not enhanced due to the cancellation<sup>9,10</sup>. In the present study, we drop ladder-type diagrams by  $\hat{V}(\omega_n)$ , which is justified when  $\omega_D \ll E_F$ <sup>9,10</sup>. For the same reason,  $\hat{V}(\omega_n)$  is absent in  $\hat{\Gamma}^s$ .

In the FLEX approximation, we obtain  $\hat{G}$  and  $\hat{\Sigma}$  self-consistently using the Dyson equation  $\hat{G}^{-1} = (\hat{G}^0)^{-1} - \hat{\Sigma}$ . In multiband systems, the FSs are modified from the original FSs due to the self-energy correction. To escape from this difficulty, we subtract the constant term  $[\hat{\Sigma}(\mathbf{k}, +i0) + \hat{\Sigma}(\mathbf{k}, -i0)]/2$  from the original self-energy, corresponding to the elimination of double-counting terms between LDA and FLEX<sup>26</sup>. Hereafter, we fix  $J/U = 1/6$ ,  $\omega_D = 0.02\text{eV}$ , and the electron filling  $n = 6.1$  except for Fig. 5. Because

of the smallness of the FSs in Fig. 1, fine  $\mathbf{k}$  meshes are required for a quantitative study. We take  $N = 128 \times 128$   $\mathbf{k}$  meshes which is four times that used in Ref.<sup>26</sup>, and 1024 Matsubara frequencies. Then, we obtain reliable numerical results for  $T \geq 0.01\text{eV}$ .

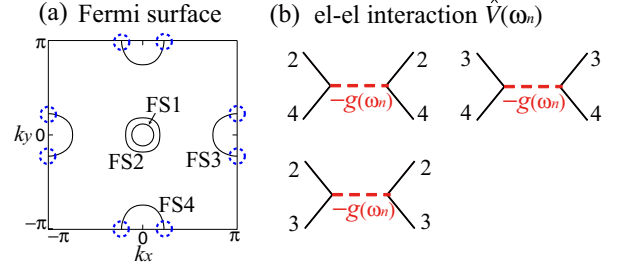


FIG. 1: (color online) (a) FSs in the unfolded zone. The dotted circles represent the cold-spot given by the orbital fluctuation theory. The cold-spot is composed of  $xz/yz$ -orbitals. (b) Phonon-mediated el-el interaction ( $\hat{V}$ ) for 2, 3, 4 orbitals.

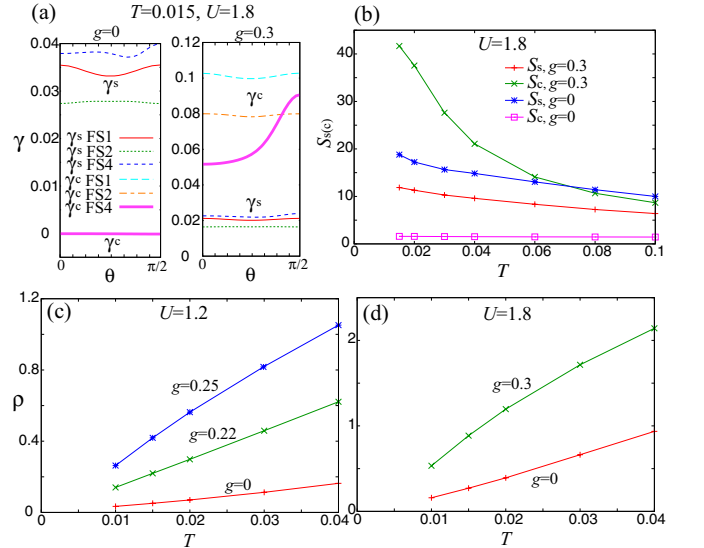


FIG. 2: (color online) (a)  $\mathbf{k}$ -dependence of  $\gamma^{s(c)}$  induced by the spin (orbital) fluctuations on each FS. Note that  $\gamma^s$  decreases with  $g$  due to the suppression of  $\hat{\chi}^s$  by  $\gamma^c$ . (b)  $T$ -dependence of  $S_{s(c)} = (1 - \alpha_{s(c)})^{-1}$ . (c), (d)  $T$ -dependence of  $\rho$ .  $\rho = 1$  corresponds to  $(\hbar a_c)/e^2 \sim 300\mu\text{cm}\Omega$  when the interlayer distance is  $a_c = 0.6\text{nm}$ .

### III. RESULT

#### A. Normal state

We begin with the electronic property in the normal state. Hereafter, the unit of energy is eV. First, we discuss the quasiparticle damping rate  $\gamma_{\mathbf{k}}$  on each FS, which is given by the imaginary part of the self-energy in the

band-diagonal representation. In Fig. 2(a),  $\gamma_{\mathbf{k}}^{s(c)}$  represents the damping due to spin (orbital) fluctuations for  $T = 0.015$  and  $U = 1.8$ , which is given by substituting  $\hat{V}^\Sigma = \frac{3}{2}\hat{\Gamma}^s\hat{\chi}^s\hat{\Gamma}^s + \frac{3}{2}\hat{\Gamma}^s(\frac{1}{2}\hat{\Gamma}^c\hat{\chi}^c\hat{\Gamma}^c + \frac{1}{2}\hat{\Gamma}^c)$  in Eq. (2). The horizontal axis is the azimuth angle for the  $\mathbf{k}$  point with the origin at the  $\Gamma(M)$  point for FS1,2 (FS4). The relationship  $\gamma_{\mathbf{k}} \approx \gamma_{\mathbf{k}}^s + \gamma_{\mathbf{k}}^c$  is satisfied since the third term in Eq. (3) is very small. We will see below that the value  $U = 1.8$  can reproduce moderate AF spin fluctuations observed in  $e$ -doped compounds, and it is consistent with  $U \sim 2$  reported by x-ray absorption spectroscopy (XAS)<sup>27</sup>.

In Fig. 2(a), the relation  $\gamma^s \gg \gamma^c$  holds for  $g = 0$ , and the momentum dependence of  $\gamma_{\mathbf{k}}^s$  on each FS is small although the AF spin correlation is well developed. The value of  $\gamma^c$  increases with  $g$ , and  $\gamma^c \sim \gamma^s$  at  $g = 0.26$ . In Fig. 2(a),  $\gamma^c \gg \gamma^s$  for  $g = 0.3$ ; the corresponding dimensionless coupling is just  $\lambda \equiv gN(0) \sim 0.2$ . Then,  $\gamma_{\mathbf{k}}^c$  on FS4 (e-pocket) is anisotropic due to the orbital dependence of  $\chi_{ll',mm'}$ , and it takes the minimum value at  $\theta \sim 0$ , where the FS is composed of 2, 3-orbitals<sup>1</sup>. This ‘‘cold-spot’’ is important for the transport phenomena. Since the cold spot is on the e-pocket, the Hall coefficient  $R_H$  will be negative, consistent with experiments<sup>22,23,28</sup>. In the case of high- $T_c$  cuprates, various non-Fermi-liquid transport phenomena (e.g., violation of Kohler’s rule) originate from the cold/hot spot structure as well as the backflow (=current vertex correction) due to the spin fluctuations<sup>29</sup>. By analogy, the appearance of the cold spot in Fig. 2(a) indicates that the orbital fluctuations are the origin of striking non-Fermi-liquid transport phenomena in iron pnictides<sup>22,23,28</sup>.

In Fig. 2(b), we show how the orbital and spin fluctuations develop as  $T$  decreases: In the FLEX, the spin (orbital) susceptibility is enhanced by the spin (orbital) Stoner enhancement factor  $S_{s(c)} = (1 - \alpha_{s(c)})^{-1}$ , where  $\alpha_{s(c)}$  is the maximum of the largest eigenvalue of  $\hat{\Gamma}^{s(c)}\hat{\chi}^{\text{irr}}(\mathbf{q}, 0)$  with respect to  $\mathbf{q}$ . Then,  $\alpha_{s,c} = 1$  corresponds to the spin/orbital order, although it is prohibited in 2D systems by the Mermin-Wagner theorem<sup>20</sup>. In the case of  $U = 1.8$  and  $g = 0$ , large  $S_s$  ( $\gtrsim 10$ ) is produced at  $\mathbf{q} \approx \mathbf{Q} \equiv (\pi, 0)$  (i.e.,  $\chi^s(\mathbf{Q}, 0) \propto S_s$ ).  $S_s$  gradually increases as  $T$  drops, which is a typical critical behavior near the AF magnetic quantum-critical-point (QCP)<sup>30</sup>. When  $g > 0$ ,  $\chi^c(\mathbf{q}, 0)$  is enhanced at  $\mathbf{q} = \mathbf{0}$  and  $\mathbf{q} = \mathbf{Q}$  almost equivalently<sup>10</sup>. At  $g = 0.3$ , large  $S_c$  ( $\gg 10$ ) is produced at  $\mathbf{q} \approx \mathbf{Q}$  or  $\mathbf{0}$ , and it increases approximately proportional to  $T^{-1}$ . Thus, it is confirmed that both ferro- and AF-orbital fluctuations show critical evolutions near the orbital QCP.

Next, we discuss the resistivity  $\rho$  due to the orbital and spin fluctuations. By neglecting the backflow, the conductivity is obtained by

$$\sigma_{xx} = \frac{e^2}{N} \sum_{\mathbf{k}, \alpha} \int_{-\infty}^{\infty} \frac{d\omega}{\pi} \left( -\frac{\partial f(\omega)}{\partial \omega} \right) |v_{\alpha, \mathbf{k}}^x G_{\mathbf{k}, \alpha}(\omega + i0)|^2, \quad (6)$$

where  $e (< 0)$  is the charge of an electron,  $\alpha$  is the band

index,  $f(\omega)$  is the Fermi distribution function,  $v_{\alpha, \mathbf{k}}^x$  is the velocity of band  $\alpha$ , and  $G_{\mathbf{k}, \alpha}(\omega + i0)$  is the retarded Green function for band  $\alpha$  in the FLEX approximation. Figure 2(c) and (d) show the obtained resistivity  $\rho = 1/\sigma_{xx}$  for  $U = 1.2$  and 1.8: In case of  $U = 1.2$ ,  $\rho$  shows a conventional sublinear (concave)  $T$ -dependence at  $g = 0$ .  $\rho$  increases with  $g$  due to the orbital fluctuations, and almost  $T$ -linear resistivity is realized at  $g = 0.22$ . At  $g = 0.25$ ,  $\rho$  shows a superlinear (convex)  $T$ -dependence. In case of  $U = 1.8$ ,  $\rho$  is linear-in- $T$  at  $g = 0$ , while it shows a clear superlinear  $T$ -dependence at  $g = 0.3$ . Thus, we stress that non-Fermi-liquid resistivity is not a direct evidence for the spin fluctuations. In  $LnFeAsO$  compounds,  $T_c$  increases as the  $As_4$  tetrahedron is close to a regular one, and the  $T$ -dependence of  $\rho$  changes from concave to convex<sup>24</sup>. Since  $g$  is maximum when the  $As_4$  tetrahedron is regular<sup>10</sup>, this experimental correlation between  $T_c$  and  $\rho(T)$  is understood in terms of the orbital fluctuation scenario. We note that non-Fermi-liquid-like frequency dependence of  $\text{Im}\Sigma(\omega)$  was recently discussed in Ref.<sup>31</sup>.

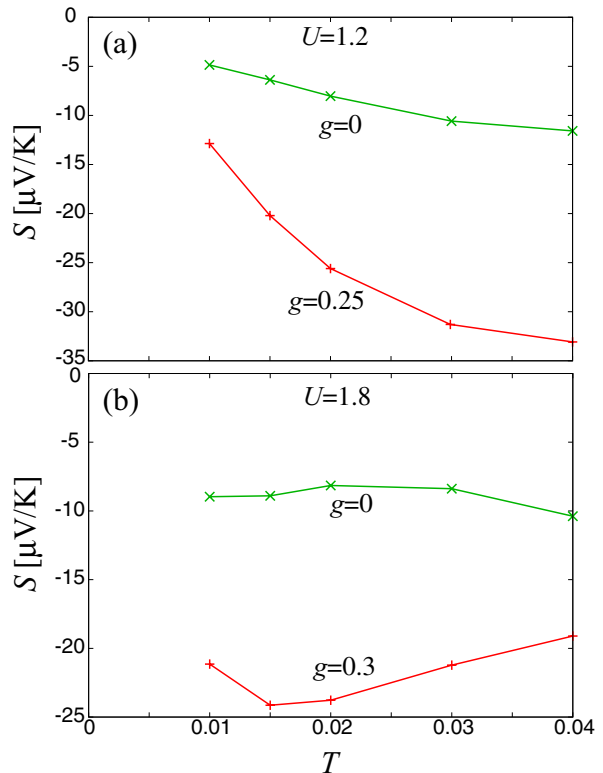


FIG. 3: (Color online)  $T$ -dependence of  $S$  for (a)  $U = 1.2$  and (b)  $U = 1.8$

Here, we study the non-Fermi-liquid-like behavior of the thermo-electric power  $S$  induced by the orbital and spin fluctuations. According to experimental results<sup>32–36</sup>,  $S$  in  $e$ -doped systems is negative below the room temperature, and  $|S|$  develops inversely proportional to the temperature till  $T^* \sim 100\text{K}$ . In optimum doped  $Ba(Fe_{1-x}Co_x)_2As_2$  peak value of  $|S| \sim 50\mu\text{V/K}$  and

$T^* \sim 130\text{K}$  are observed.<sup>36</sup> Similar behaviors are also observed in high- $T_c$  cuprates with the strong AF spin fluctuation. Thus, such remarkable non-Fermi-liquid behaviors in iron pnictides are expected to be realized by the orbital and spin fluctuations.

Since the effect of backflow is small for  $S$ ,<sup>37</sup> we calculate  $S$  by neglecting the backflow as follows

$$S = \frac{e}{\sigma_{xx}TN} \sum_{\mathbf{k},\alpha} \int_{-\infty}^{\infty} \frac{d\omega}{\pi} \left( -\frac{\partial f(\omega)}{\partial \omega} \right) \omega |v_{\alpha,\mathbf{k}}^x G_{\mathbf{k},\alpha}(\omega + i0)|^2. \quad (7)$$

The obtained  $T$ -dependence of  $S$  is shown in Fig. 3. In the case of  $U = 1.2$ , Fermi-liquid-like behavior ( $S \propto T$ ) is obtained for  $g = 0$ , where both the spin and orbital fluctuations are weak. For  $g = 0.25$ , where the orbital fluctuation is strong,  $|S|$  becomes larger than that for  $g = 0$ , and the deviation from the Fermi-liquid-like behavior is realized. In the case of  $U = 1.8$ , where spin fluctuation is strong, non-Fermi-liquid-like behavior is obtained as shown in Fig. 3(b). For  $g = 0$ , the value of  $|S|$  is small and almost independent of  $T$ . On the other hand,  $|S|$  is drastically enhanced, and shows the peak at  $T^* \sim 150\text{K}$  for  $g = 0.3$ , where both the spin and orbital fluctuation are strong. The obtained result for  $U = 1.8$  and  $g = 0.3$  is consistent with experiments.<sup>32-36</sup> In the following, we explain why the absolute value of  $S$  becomes large for large value of  $g$ . Since  $v_{\alpha,\mathbf{k}} \sim 1/N_{\alpha}(\omega)$  at  $\omega = \varepsilon_{\mathbf{k}}^{\alpha}$ , where  $N_{\alpha}$  and  $\varepsilon_{\mathbf{k}}^{\alpha}$  are the density of state and the dispersion on band  $\alpha$ , respectively,  $S$  is rewritten as

$$\begin{aligned} S &\propto \frac{e}{\sigma_{xx}T} \sum_{\alpha} \int_{-\infty}^{\infty} d\omega \frac{z_{\alpha}\omega}{N_{\alpha}(\omega)\gamma_{\alpha}(\omega)} \left( -\frac{\partial f(\omega)}{\partial \omega} \right) \\ &\propto \frac{-eT}{\sigma_{xx}} \sum_{\alpha} z_{\alpha} \frac{\partial}{\partial \omega} \left( \frac{1}{N_{\alpha}(\omega)\gamma_{\alpha}(\omega)} \right)_{\omega=0}, \end{aligned} \quad (8)$$

where  $z_{\alpha} = \left(1 - \frac{\partial \Sigma_{\alpha}(\omega)}{\partial \omega}\right)_{\omega=0}^{-1}$  and  $\gamma_{\alpha}$  are the renormalization factor and the quasiparticle damping on band  $\alpha$ , respectively. When the orbital fluctuations are weak,  $S$  takes small and negative value because  $\frac{\partial}{\partial \omega} N_{\alpha} > 0$  is satisfied on the e-pocket (cold spots). In the case of strong orbital fluctuation with large value of  $g$ ,  $S$  is still negative while the absolute value is much enhanced. due to the large value of  $\frac{\partial}{\partial \omega} \gamma_{\alpha} > 0$  at the cold spots on e-pocket shown in Fig. 2(a). Thus, the orbital fluctuation plays an important role in enhancing the absolute value of  $S$  and reproducing the experimental results. We stress that result for  $U = 1.8$  and  $g = 0.3$  well reproduce the experimental behaviors of  $S$  in optimum doped  $\text{Ba}(\text{Fe}_{1-x}\text{Co}_x)_2\text{As}_2$ .<sup>36</sup>

In the present FLEX approximation, almost isotropic damping is obtained for  $U = 1.8$  and  $g = 0$ , as shown in Fig. 2(a). In contrast, Kemper *et al.*<sup>38</sup> reported a clear hot/cold spot structure due to the spin fluctuation using the RPA self-energy (self-inconsistent FLEX approximation). This difference would come from the presence (absence) of self-consistency in the former (latter) calculation. Kemper *et al.*<sup>38</sup> also reported interesting doping de-

pendence of the sign of Hall coefficient  $R_H$ . However, current vertex corrections would be necessary to reproduce the magnitude and  $T$ -dependence of  $R_H$  appropriately.<sup>39</sup>

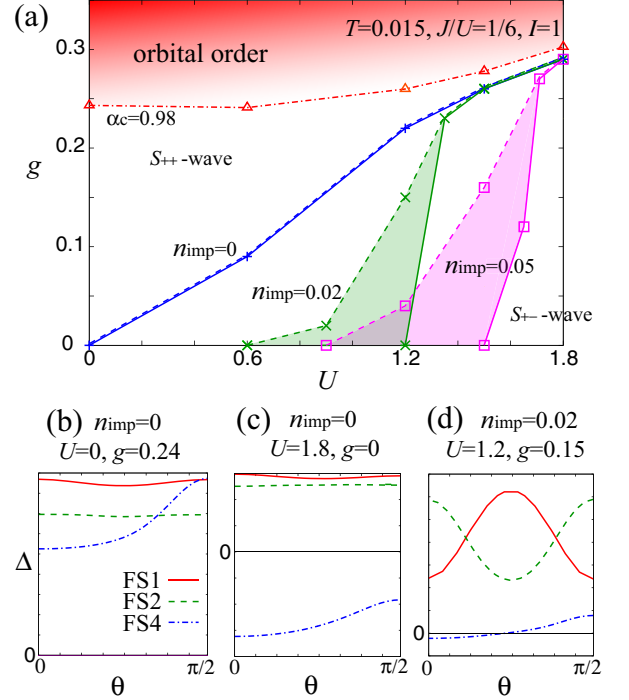


FIG. 4: (Color online) (a)  $U$ - $g$  phase diagram given by solving the linearized Eliashberg equation at  $T = 0.015$ . Nodal  $s$ -wave gap state is obtained in the shaded area for  $n_{\text{imp}} = 0.02$  and  $0.05$ , and solid lines (dotted lines) represent the boundary between fully-gapped  $s_{+-}$ -wave ( $s_{++}$ -wave) state. Dashed-dotted line denotes  $\alpha_c = 0.98$ . (b)  $s_{++}$ -wave gap ( $\lambda_E = 0.59$ ) for  $U = 0$  and  $g = 0.24$ . (c)  $s_{+-}$ -wave gap ( $\lambda_E = 0.49$ ) for  $U = 1.8$  and  $g = 0$  and. (d) Nodal  $s$ -wave gap ( $\lambda_E = 0.28$ ) for  $U = 1.2$  and  $g = 0.15$ .

## B. SC state

Next, we discuss the SC state. In the presence of dilute impurities ( $n_{\text{imp}} \ll 1$ ), the linearized Eliashberg equation in the orbital basis is<sup>9</sup>

$$\begin{aligned} \lambda_E \Delta_{ll'}(k) &= -\frac{T}{N} \sum_{k', m_i} W_{lm_1, m_4 l'}(k - k') G'_{m_1 m_2}(k') \\ &\quad \times \Delta_{m_2 m_3}(k') G'_{m_4 m_3}(-k') + \delta \Sigma_{ll'}^a(\epsilon_n), \end{aligned} \quad (9)$$

where  $\Delta_{ll'}(k)$  is the gap function and  $\lambda_E$  is the eigenvalue that reaches unity at  $T = T_c$ .  $\delta \hat{\Sigma}^a$  represents the impurity-induced gap function.  $(\hat{G}')^{-1} = (\hat{G})^{-1} - \delta \hat{\Sigma}^n$ , where  $G$  is the Green function given by Eq. (2), and  $\delta \hat{\Sigma}^n$  is the impurity-induced normal self-energy. The pairing interaction  $\hat{W}$  in Eq. (9) is

$$\hat{W}(q) = \frac{3}{2} \hat{\Gamma}^s \hat{\chi}^s(q) \hat{\Gamma}^s - \frac{1}{2} \hat{\Gamma}^c \hat{\chi}^c(q) \hat{\Gamma}^c + \frac{1}{2} \hat{\Gamma}^s - \frac{1}{2} \hat{\Gamma}^c, \quad (10)$$

where  $\hat{\chi}^{s,c}$  is given by the FLEX approximation for  $n_{\text{imp}} = 0$ , because of the fact that the fully self-consistent FLEX with impurity-induced self-energy leads to unphysical reduction in  $\chi^s$ , unless vertex correction is taken into account<sup>29</sup>. The first (second) term in Eq. (10) works to set  $\Delta_{\text{FS1,2}} \cdot \Delta_{\text{FS3,4}} < 0$  ( $> 0$ ).

In the  $T$ -matrix approximation,  $\delta\hat{\Sigma}^{n,a}$  is given as

$$\delta\Sigma_{ij}^n(\epsilon_n) = n_{\text{imp}}T_{ij}(\epsilon_n), \quad (11)$$

$$\delta\Sigma_{ij}^a(\epsilon_n) = n_{\text{imp}} \sum_{lm} T_{il}(\epsilon_n) f_{lm}(\epsilon_n) T_{jm}(-\epsilon_n), \quad (12)$$

where  $T_{ij}(\epsilon_n) \equiv I(1 - I\hat{g}(\epsilon_n))^{-1}$  is the  $T$ -matrix in the normal state<sup>15</sup>;  $\hat{g}(\epsilon_n) \equiv \frac{1}{N} \sum_{\mathbf{k}} \hat{G}_{\mathbf{k}}(\epsilon_n)$  is the local normal Green function, and  $I$  is the local impurity potential that is diagonal in the orbital basis. We put  $I = 1$  hereafter. In Eq. (12),  $f_{ij}(\epsilon_n) = \frac{1}{N} \sum_{\mathbf{k}, lm} G_{il}(\mathbf{k}) \Delta_{lm}(\mathbf{k}) G_{jm}(-\mathbf{k})$  is the linearized local anomalous Green function.

In Fig. 4(a), we show the  $U$ - $g$  phase diagram obtained by the FLEX approximation. The dashed-dotted line represents the condition  $\alpha_c = 0.98$  at  $T = 0.015$ , corresponding to  $g = 0.25 \sim 0.3$ . (In the RPA, the same condition is satisfied for  $g = 0.21 \sim 0.23$ .<sup>10</sup>) Therefore, substantial orbital fluctuations emerge for  $\lambda = gN(0) \lesssim 0.2$  even if the self-energy correction is taken into account. On the other hand,  $\alpha_s = 0.95$  (0.92) for  $U = 1.8$  and  $g = 0$  (0.3) in the FLEX approximation, although  $U_{\text{cr}} = 1.25$  for  $\alpha_s = 1$  in the RPA. Thus, the renormalization in  $\alpha_s$  is much larger than that in  $\alpha_c$ , because of the difference in the coefficients (in factor 3) between the first and the second terms in Eq. (3).

Next, we solve Eq. (9) with high accuracy using the Lanczos method at  $T = 0.015$ . Then, the  $s_{++}$ -wave gap function is obtained around the line  $\alpha_c = 0.98$ ; Figure 4(b) shows the  $s_{++}$ -wave gap for  $g = 0.24$  and  $U = 0$  ( $\lambda_E = 0.59$ ). On the other hand,  $s_{\pm}$ -wave gap is obtained when  $g$  is sufficiently small; Figure 4(c) shows the  $s_{\pm}$ -wave gap for  $U = 1.8$  and  $g = 0$  ( $\lambda_E = 0.49$ ). When  $n_{\text{imp}} = 0$ , the gap function changes from (b) to (c) discontinuously on the phase boundary in Fig. 4(a), as found in Ref.<sup>10</sup>. When  $n_{\text{imp}} \geq 0.02$ , however, the gap function changes smoothly during the crossover. Then, line-nodes inevitably appear on FS3,4 in the shaded area in Fig. 4(a); Figure 4(d) shows the nodal  $s$ -wave gap for  $U = 1.2$ ,  $g = 0.15$  and  $n_{\text{imp}} = 0.02$  ( $\lambda_E = 0.28$ ). Thus, both regions for  $s_{++}$ -wave and nodal  $s$ -wave states are extended by a small amount of impurities, although  $\lambda_E$  for the latter state is reduced by impurities. A nodal  $s$ -wave solution at  $n_{\text{imp}} = 0$  with larger  $\lambda_E$  may be obtained by considering a 3D nodal-line structure in a 3D tight-binding model<sup>40</sup>.

Here, we discuss that line nodes originate from the competition between the orbital and spin fluctuations: The electrons at  $\theta \sim 0$  ( $\pi/2$ ) on FS4 are composed of orbital 2,3 (4). Since the orbital 4 is absent in FS1,2, the nesting-driven spin correlation between the orbital 2,3 on FS1,2 and the orbital 4 on FS3,4 is weak. (That is,  $\chi_{24,42}^s(\mathbf{Q}) \ll \chi_{22,22}^s(\mathbf{Q})$ .) On the other hand,

both  $\chi_{24,42}^c(\mathbf{Q})$  and  $\chi_{22,22}^c(\mathbf{Q})$  develop well<sup>9-11</sup>. Therefore, when orbital and spin fluctuations are comparable,  $\Delta_{\text{FS1,2}} \cdot \Delta_{\text{FS4}}$  is negative (positive) at  $\theta \sim 0$  ( $\pi/2$ ) due to the orbital-dependences of the spin and orbital susceptibilities.

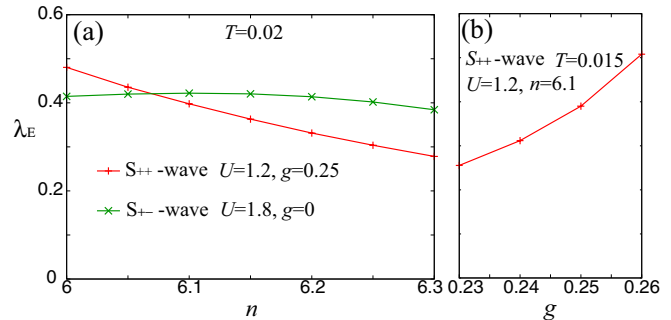


FIG. 5: (Color online) (a)  $n$  dependence of  $\lambda_E$  for  $s_{++}$ - and  $s_{+-}$ -wave states at  $T = 0.02$  and  $n_{\text{imp}} = 0$ . (b)  $g$  dependence of  $\lambda_E$  for  $s_{++}$ -wave state at  $T = 0.015$  and  $n_{\text{imp}} = 0$ .

In Fig. 5(a), we show the filling dependence of  $\lambda_E$  for the  $s_{++}$ -wave state ( $U = 1.2, g = 0.25$ ), and that for the  $s_{+-}$ -wave state ( $U = 1.8, g = 0$ ). We note that FS1,2 disappear for  $n > 6.3$ . The value of  $\lambda_E$  for the  $s_{++}$ -wave state decreases monotonically with  $n$ , while  $\lambda_E$  for the  $s_{+-}$ -wave state is rather insensitive to  $n$ , maybe because the temperature,  $T = 0.02$ , is rather high. Figure 5(b) shows that  $\lambda_E$  for the  $s_{++}$ -wave state ( $U = 1.2, n = 6.1$ ) increases with  $g$ .

#### IV. CONCLUSION

We performed the FLEX approximation in the multi-orbital Hubbard model including the charge quadrupole interaction for iron pnictides. It was confirmed that the orbital-fluctuation-mediated  $s_{++}$ -wave state is realized by small  $e$ -ph interaction  $g$ . As increasing the value of  $g$ , both the  $T_c$  of the  $s_{++}$ -wave state and the resistivity  $\rho$  are increased, and the latter changes from  $T$ -concave to  $T$ -convex. This correlation between  $T_c$  and  $\rho$  is consistent with experiment<sup>24</sup>. Moreover, the obtained thermoelectric power  $S$  is a large negative value due to cold spots on the  $e$ -pocket, when the orbital fluctuation is dominant. The large negative value of  $S$  is consistent with experiments<sup>32-36</sup>. We note that the region of  $s_{++}$ -wave or nodal  $s$ -wave states is enlarged in the presence of a small amount of impurities. Thus, the present orbital fluctuation scenario presents a unified explanation for both normal and SC electronic states.

#### Acknowledgments

We are grateful to M. Sato, Y. Kobayashi, Y. Matsuda, T. Shibauchi, D.S. Hirashima, Y. Tanaka, K. Yamada,

and F.C. Zhang for valuable discussions. This study has been supported by Grants-in-Aid for Scientific Research

from MEXT of Japan, and by JST, TRIP.

- 
- <sup>1</sup> K. Kuroki, S. Onari, R. Arita, H. Usui, Y. Tanaka, H. Kontani, and H. Aoki, *Phys. Rev. Lett.* **101**, 087004 (2008); K. Kuroki, H. Usui, S. Onari, R. Arita, and H. Aoki, *Phys. Rev. B* **79**, 224511 (2009).
- <sup>2</sup> I. I. Mazin, D. J. Singh, M. D. Johannes, and M. H. Du, *Phys. Rev. Lett.* **101**, 057003 (2008).
- <sup>3</sup> V. Cvetkovic and Z. Tesanovic, *Europhys. Lett.* **85**, 37002 (2009).
- <sup>4</sup> P. J. Hirschfeld, M. M. Korshunov, and I. I. Mazin, *Rep. Prog. Phys.* **74**, 124508 (2011).
- <sup>5</sup> A. V. Chubukov, e-print arXiv:1110.0052.
- <sup>6</sup> Y. Nakai, T. Iye, S. Kitagawa, K. Ishida, H. Ikeda, S. Kasahara, H. Shishido, T. Shibauchi, Y. Matsuda, T. Terashima, *Phys. Rev. Lett.* **105**, 107003 (2010).
- <sup>7</sup> T. Nakano, N. Fujiwara, K. Tatsumi, H. Okada, H. Takahashi, Y. Kamihara, M. Hirano, and H. Hosono, *Phys. Rev. B* **81**, 100510(R) (2010).
- <sup>8</sup> S. Onari and H. Kontani, e-print arXiv:1203.2874.
- <sup>9</sup> H. Kontani and S. Onari, *Phys. Rev. Lett.* **104**, 157001 (2010).
- <sup>10</sup> T. Saito, S. Onari, and H. Kontani, *Phys. Rev. B* **82**, 144510 (2010).
- <sup>11</sup> T. Saito, S. Onari, and H. Kontani, *Phys. Rev. B* **83**, 140512(R) (2011).
- <sup>12</sup> H. Kontani, T. Saito, and S. Onari, *Phys. Rev. B* **84**, 024528 (2011).
- <sup>13</sup> C.-H. Lee, A. Iyo, H. Eisaki, H. Kito, M. T. Fernandez-Diaz, T. Ito, K. Kihou, H. Matsuhata, M. Braden, and K. Yamada, *J. Phys. Soc. Jpn.* **77**, 083704 (2008); Y. Mizuguchi, Y. Hara, K. Deguchi, S. Tsuda, T. Yamaguchi, K. Takeda, H. Kotegawa, H. Tou, and Y. Takano, *Supercond. Sci. Technol.* **23**, 054013 (2010).
- <sup>14</sup> M. Yoshizawa, D. Kimura, T. Chiba, A. Ismayil, Y. Nakanishi, K. Kihou, C.-H. Lee, A. Iyo, H. Eisaki, M. Nakajima, and S. Uchida, *J. Phys. Soc. Jpn.* **81**, 024604 (2012).
- <sup>15</sup> S. Onari and H. Kontani, *Phys. Rev. Lett.* **103**, (2009) 177001.
- <sup>16</sup> A. Kawabata, S. C. Lee, T. Moyoshi, Y. Kobayashi and M. Sato, *J. Phys. Soc. Jpn.* **77**, 103704 (2008).
- <sup>17</sup> Y. Nakajima, T. Taen, Y. Tsuchiya, T. Tamegai, H. Kitamura, and T. Murakami, *Phys. Rev. B* **82**, 220504 (2010).
- <sup>18</sup> S. Onari, H. Kontani, and M. Sato, *Phys. Rev. B* **81**, 060504(R) (2010); S. Onari and H. Kontani, *Phys. Rev. B* **84**, 144518 (2011).
- <sup>19</sup> N. E. Bickers, and D. J. Scalapino, *Ann. Phys. (N.Y.)* **193**, 206 (1989).
- <sup>20</sup> H. Kontani and M. Ohno, *Phys. Rev. B* **74**, 014406 (2006).
- <sup>21</sup> The present paper is a full paper version of S. Onari and H. Kontani, e-print arXiv:1009.3882.
- <sup>22</sup> R. H. Liu, G. Wu, T. Wu, D. F. Fang, H. Chen, S. Y. Li, K. Liu, Y. L. Xie, X. F. Wang, R. L. Yang, L. Ding, C. He, D. L. Feng, and X. H. Chen, *Phys. Rev. Lett.* **101**, 087001 (2008).
- <sup>23</sup> S. Kasahara, T. Shibauchi, K. Hashimoto, K. Ikada, S. Tonegawa, R. Okazaki, H. Shishido, H. Ikeda, H. Takeya, K. Hirata, T. Terashima, and Y. Matsuda, *Phys. Rev. B* **81**, 184519 (2010).
- <sup>24</sup> K. Miyazawa, K. Kihou, P. M. Shirage, C.-H. Lee, H. Kito, H. Eisaki, and A. Iyo, *J. Phys. Soc. Jpn.* **78**, 034712 (2010); S. Ishida, M. Nakajima, Y. Tomioka, T. Ito, K. Miyazawa, H. Kito, C. H. Lee, M. Ishikado, S. Shamoto, A. Iyo, H. Eisaki, K. M. Kojima, and S. Uchida, *Phys. Rev. B* **81**, 094515 (2010).
- <sup>25</sup> T. Takimoto, T. Hotta, and K. Ueda, *Phys. Rev. B* **69**, 104504 (2004).
- <sup>26</sup> H. Ikeda, R. Arita, and J. Kunes, *Phys. Rev. B* **81**, 054502 (2010).
- <sup>27</sup> W. L. Yang *et al.*, *Phys. Rev. B* **80**, 014508 (2009).
- <sup>28</sup> S. C. Lee, A. Kawabata, T. Moyoshi, Y. Kobayashi, and M. Sato, *J. Phys. Soc. Jpn.* **78**, 043703 (2009).
- <sup>29</sup> H. Kontani, *Rep. Prog. Phys.* **71** (2008) 026501.
- <sup>30</sup> T. Moriya and K. Ueda, *Adv. Phys.* **49**, 555 (2000).
- <sup>31</sup> W. C. Lee and P. W. Phillips, e-print arXiv:1110.5917v2.
- <sup>32</sup> M. A. McGuire *et al.*, *Phys. Rev. B* **78**, 094517 (2008).
- <sup>33</sup> M. Tropeano, C. Fanciulli, C. Ferdeghini, D. Marre, A. S. Siri, M. Putti, A. Martinelli, M. Ferretti, A. Palenzona, M. R. Cimberle, C. Mirri, S. Lupi, R. Sopracase, P. Calvani, and A. Perucchi, *Supercond. Sci. Technol.* **22**, 034004 (2009).
- <sup>34</sup> S. J. Singh, J. Prakash, S. Patnaik, A. K. Ganguli *Supercond. Sci. Technol.* **22**, 045017 (2009).
- <sup>35</sup> V. P. S. Awana, R. S. Meena, A. Pal, A. Vajpayee, K. V. R. Rao, and H. Kishan, *Eur. Phys. J. B* **79**, 139 (2011).
- <sup>36</sup> E. D. Mun, S. L. Bud'ko, N. Ni, A. N. Thaler, and P. C. Canfield, *Phys. Rev. B* **80**, 054517 (2009).
- <sup>37</sup> H. Kontani, *J. Phys. Soc. Jpn.* **70**, 2840 (2001).
- <sup>38</sup> A. F. Kemper, M. M. Korshunov, T. P. Devereaux, J. N. Fry, H-P. Cheng, P. J. Hirschfeld, *Phys. Rev. B* **83**, 184516 (2011).
- <sup>39</sup> H. Kontani, K. Kanki, and K. Ueda, *Phys. Rev. B* **59**, 14723 (1999).
- <sup>40</sup> I.I. Mazin, T. P. Devereaux, J. G. Analytis, J. -H. Chu, I. R. Fisher, B. Muschler, and R. Hackl, *Phys. Rev. B* **82**, 180502(R) (2010).